

ANL/Phy/CP-101895

Ternary particles with extreme N/Z ratios from neutron-induced fission

Ulli Köster

Technische Universität München, Physik-Department, 85748 Garching, Bavaria

Herbert Faust, Thomas Friedrichs, Stephan Oberstedt

Institut Laue Langevin, 38042 Grenoble, France

Gabriele Fioni

CEA Saclay, DSM/DAPNIA/SPHN, 91191 Gif-sur-Yvette, France

Martin Groß

*Ludwig-Maximilians-Universität München, Sektion für Physik,
85748 Garching, Bavaria*

Irshad Ahmad

Argonne National Laboratory, Physics Division, Argonne, Illinois 60439

The existing ternary fission models can well reproduce the yields of the most abundant light charged particles. However, these models tend to significantly overestimate the yields of ternary particles with an extreme N/Z ratio: ^3He , ^{11}Li , ^{14}Be , etc. The experimental yields of these isotopes were investigated with the recoil separator LOHENGRIN down to a level of 10^{-10} per fission. Results from the fissioning systems $^{233}\text{U}(n_{\text{th}},f)$, $^{235}\text{U}(n_{\text{th}},f)$, $^{239}\text{Pu}(n_{\text{th}},f)$, $^{241}\text{Pu}(n_{\text{th}},f)$ and $^{245}\text{Cm}(n_{\text{th}},f)$ are presented and the implications for the ternary fission models are discussed.

Introduction

Ternary fission^a has been studied for the past 50 years^{1,2}. There is clear evidence that most of the ternary particles (TP) are created in the neck region between the two fission fragments (see e.g.³). The geometry of the scission configuration should manifest itself in the abundance and kinetic energy distribution of the TP. Thus, a detailed measurement of the latter can give a possibility to deduce information on the scission configuration. In the last few years the amount of measured data on TP yields and energy distributions from various fissioning systems increased considerably. For a general review on the experimental techniques, results and conclusions see e.g. ref.³. Here we will concentrate on data of exotic isotopes with an extreme N/Z ratio.

^aFor brevity the expression "ternary fission" will be used synonymously for the more correct "light charged particle accompanied fission."

RECEIVED
JUN 05 2000
OSTI

DISCLAIMER

This report was prepared as an account of work sponsored by an agency of the United States Government. Neither the United States Government nor any agency thereof, nor any of their employees, make any warranty, express or implied, or assumes any legal liability or responsibility for the accuracy, completeness, or usefulness of any information, apparatus, product, or process disclosed, or represents that its use would not infringe privately owned rights. Reference herein to any specific commercial product, process, or service by trade name, trademark, manufacturer, or otherwise does not necessarily constitute or imply its endorsement, recommendation, or favoring by the United States Government or any agency thereof. The views and opinions of authors expressed herein do not necessarily state or reflect those of the United States Government or any agency thereof.

DISCLAIMER

Portions of this document may be illegible in electronic image products. Images are produced from the best available original document.

Ternary fission models

Most models which are used to describe binary fission (e.g. ^{4,5}) cannot be applied directly for ternary fission. Typically the parameterization of the scission configuration does not provide enough degrees of freedom to describe the development of a third particle in the neck region.

There is still no theory which could reproduce the individual yields and energy distributions of ternary fission fragments from first principles. Several models deal only with the abundance of long range alphas (LRA) per binary fission or provide a qualitative discussion of TP emission without treating individual yields or energy distributions. In the following some models will be presented which describe the relative emission probabilities of various TP in different fissioning systems.

Valskii fit formula: Valskii ⁶ gave a pure interpolation formula without assuming any special scission configuration. Four free parameters were fitted to reproduce the then known ternary yields of ²³³U(*n*_{th},*f*), ²³⁵U(*n*_{th},*f*) and ²³⁹Pu(*n*_{th},*f*). The total yield of each isotope was obtained by a statistical sum over all particle stable levels of the isotope.

Double-neck-rupture model: Rubchenya and Yavshits proposed a statistical model of a double neck rupture ⁷. A ternary proto-particle with mass ≈ 10 is created between both fragments in a compact collinear configuration. The heavy fragment mass is fixed to 140. The ternary proto-particle is thought to stay in close contact with the light fission fragment for a while and exchange nucleons. The proton and neutron numbers are changed to that of the finally ejected particle.

In a more recent version of the double-neck-rupture model ⁸, the ternary yields were averaged over the contributions of all mass splits, weighted with the pre-neutron-emission fragment yields from binary fission.

Modified double-neck-rupture model: Baum et al. proposed a fundamental modification of the double neck rupture model ^{9,10}. They omitted the idea of a proto-particle and calculated directly the Q-value of the reaction. The mass split is chosen to obtain the highest Q-value. A triangular scission configuration is assumed where the TP is emitted off-axis about midway between both fragments. The tip distance between TP and light fragment is just half of the tip distance between both fragments. This scission configuration provides also the start conditions for trajectory calculations. The tip distance is adapted to reproduce the measured mean kinetic energies of the heavier TP ($Z \geq 3$).

“Transition energy” model: In a model proposed by Pik-Pichak¹¹ the relative emission probability of a TP is related to a relative “transition energy” given by the difference of reaction Q-value and Coulomb energy. A collinear scission configuration of nearly touching fragments is used. The heavy fragment (¹³²Sn or a nucleus in its close vicinity) and the TP are assumed to be spherical while the light fragment is deformed, which is reflected in a modified radius parameter.

Boltzmann model: Faust and Bao¹² related the TP yields by a Boltzmann ansatz to the energy necessary to create the ternary scission configuration, i.e. the sum of the Coulomb energy (calculated for a compact triangular scission configuration with three nearly touching spheres), the reaction Q-value (calculated from the mass excesses of the compound nucleus and all involved fragments and increased by 6 MeV neutron binding energy in the case of neutron-induced fission) and an additional correction energy accounting for the loss of pairing energy of the TP. The latter is individually fitted^b for even-even, even-odd, odd-even and odd-odd TP.

The nuclear temperature is assumed to be identical to the one used in a similar model for binary fission¹³. All possible fission mass splits are weighted with the known binary mass yields and summated.

Extended Halpern model: The extended Halpern model^{14,15} was developed at the Tübingen university following the ideas of Halpern¹⁶. He proposed that ternary fission mainly occurs in very elongated scission configurations where the high stored deformation energy is released at the moment of scission (“sudden snapping-in of the neck”) and allows the emission of a third particle. The ternary scission configuration is obtained by placing a TP in between both fragments while keeping the center-of-mass of the total system fixed. The “energy costs” for such a configuration compared with a binary configuration are calculated and averaged over all individual mass splits using the known binary yields for weighting. The tip distance in the binary configuration is calculated from the minimum kinetic energies of the fragments observed in binary fission.

^bIn total a dozen of free parameters are used to reproduce the measured yields from ²⁴¹Am(2n,f). The same parameters are used for all fissioning systems.

Common parameterization

The presented models use quite different ideas to derive or illustrate a relation for the TP yields, but it is remarkable that all of them (except for the Valskii fit formula) formally have the same simple dependence:

$$y = C \exp(-\Delta E/T). \quad (1)$$

The energy parameter ΔE describes the effort of the fissioning system to emit a TP. It is mainly composed of the Q-value and the Coulomb energy of the scission configuration. The main difference of the models lies in the geometry of the scission configuration which in turn strongly influences the Coulomb energy term in ΔE . The second difference between the models is the interpretation of the parameter T describing the ability to access energetically unfavorable scission configurations. While some models explicitly introduce it as nuclear temperature of the fissioning system, others explicitly claim it is not a temperature.

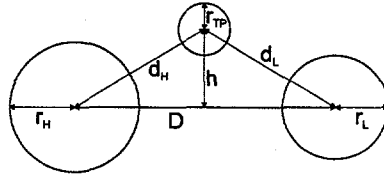


Figure 1: Universal parameterization for the scission configuration of most ternary fission models.

Figure 1 shows a universal parameterization of the scission configuration. The parameters of the individual models are summarized in table 1. The interfragment distance of most models is in reasonable agreement with a value of 21 to 22 fm as determined by trajectory calculations for long range alpha accompanied fission¹⁷. Only the Faust formula has a very compact configuration with a minimum tip distance even smaller than in compact binary fission¹⁸. Therefore the chosen scission configuration is prohibited by energy conservation and has rather to be regarded as a “virtual” state.

All models use some free parameters which are fitted to reproduce experimentally determined yield values. This procedure will always result in a more or less good reproduction of the most abundant yields, see figure 2. However, larger deviations between the models occur for rare TP, i.e. very heavy ones ($A_{TP} \gg 20$) and “exotic” isotopes with an extreme N/Z ratio (^3He , ^{11}Li , etc.). The measurement of these TP yields is a good way to probe the predictions of the different models.

The yields of the heavier TP are affected by both the Q-value and the Coulomb energy term, while the yields of lighter exotic nuclei depend mainly

Table 1: Parameters as defined in figure 1 for the case of ^{10}Be accompanied fission of $^{235}\text{U}(n_{\text{th}},f)$. The models are listed as above. For models using an average over many mass splits only a typical example close to the peak of the fragment mass distribution is given.

Model (ref.)	Heavy fragment	Light fragment	D fm	d_L fm	d_H fm	h fm	T MeV
7	^{140}Cs	^{86}As	≈ 25	11.2	≈ 13.8	0	2.1
8,19	^{132}Sn	^{94}Sr	23.6	11.3	12.3	0	2.19
10	^{132}Sn	^{94}Sr	22.6	13.6	14.2	7.5	1.91
11	^{132}Sn	^{94}Sr	22.9	12.8	10.1	0	2.1
12	^{132}Sn	^{94}Sr	13.4	9.9	10.5	7.7	1.3
15	^{132}Sn	^{94}Sr	22.4	10.8	11.6	0	3.1

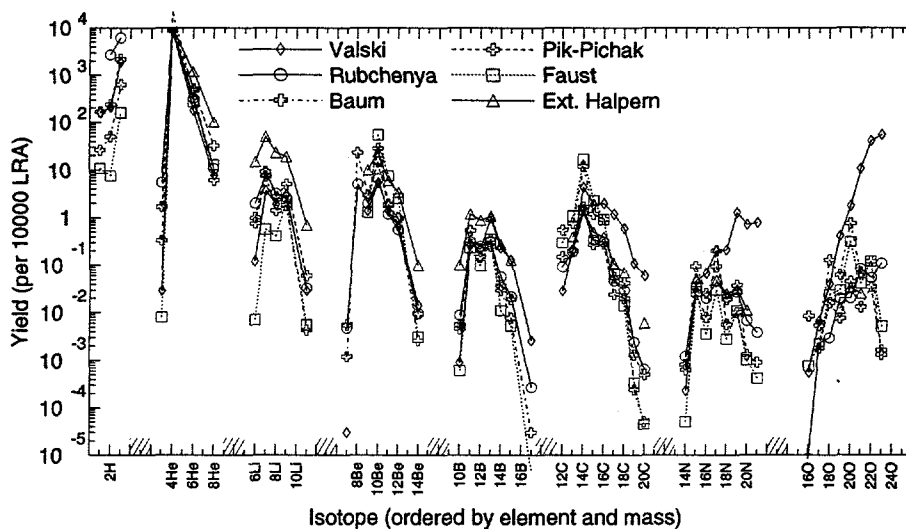


Figure 2: Ternary fission yields for $^{235}\text{U}(n_{\text{th}},f)$, calculated with different models. Here, and in the following yield comparisons the isotopes of each element are grouped together in a series. From left to right: $^1\text{--}^3\text{H}$, $^3\text{--}^8\text{He}$, $^6\text{--}^{11}\text{Li}$, $^7\text{--}^{14}\text{Be}$, $^{10}\text{--}^{17}\text{B}$, $^{12}\text{--}^{20}\text{C}$, $^{14}\text{--}^{21}\text{N}$ and $^{15}\text{--}^{24}\text{O}$.

on the Q-value. Exemplary this dependence is shown in figures 3 and 4. The most abundant particle-stable isotopes of the elements hydrogen to oxygen are plotted. The calculation was performed with the Boltzmann model, but all other models show qualitatively the same dependence: with slightly varying temperature the yields of less abundant nuclei change by more than one order of magnitude.

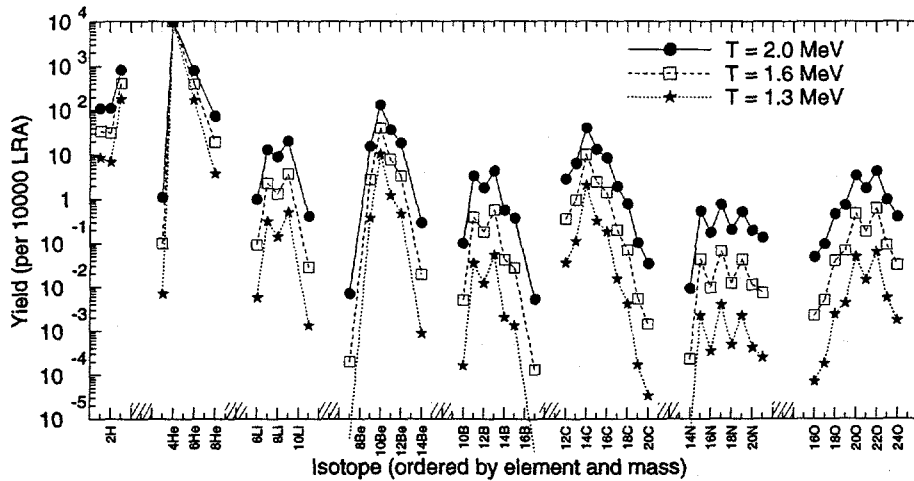


Figure 3: Ternary fission yields for $^{241}\text{Pu}(n_{\text{th}}, f)$, calculated with different temperatures in the "Faust formula".

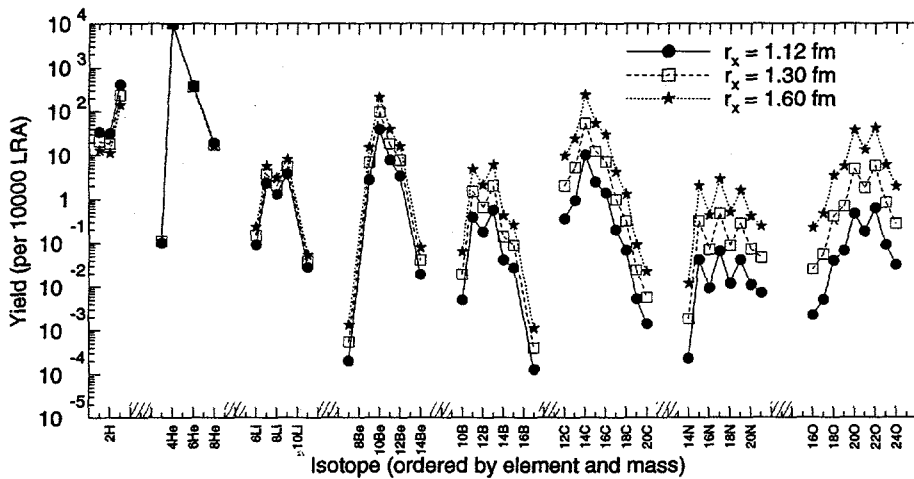


Figure 4: Ternary fission yields for $^{241}\text{Pu}(n_{\text{th}}, f)$, calculated with different interfragment distances in the "Faust formula". r_x is the main radius parameter in the Bass formula²⁰. The scale is identical to figure 2.

However, when changing the shape of the scission configuration from a compact to an elongated one, the yields of the light rare isotopes stay practically constant, while the yields of heavier elements increase considerably. With

increasing distance of the fragments, the Coulomb energy term is reduced, thus affecting less the "energy costs" of the heavy TP production.

Thus, yield data of both, the light exotic and the heavy TP, is required to determine the two main model parameters: "temperature" and "elongation".

Experimental results

Dedicated measurements of the heavy TP yields were mainly performed by the Tübingen group^{3,21,22,23}. In the following only the results on light exotic nuclei are reported. All experiments were performed with the recoil separator LOHENGRIN at the high-flux reactor of the Institut Laue Langevin. The experimental technique and the data evaluation are presented together with all measured data of the system $^{241}\text{Pu}(n_{\text{th}},f)$ in ref.²⁴. The yield values for $^{239}\text{Pu}(n_{\text{th}},f)$ were taken from²⁵ and those for $^{233}\text{U}(n_{\text{th}},f)$, $^{235}\text{U}(n_{\text{th}},f)$ and $^{245}\text{Cm}(n_{\text{th}},f)$ from²⁶.

Yields of neutron-deficient nuclei

Compared with neutron-rich nuclei, the measurement of rare neutron-deficient^c nuclei is generally more difficult with the LOHENGRIN spectrometer. In spectra of fully stripped neutron-rich nuclei always isobars with the same ionic charge state but higher Z are present on the $\Delta E/E$ plots and allow a direct monitoring of the experimental conditions. Any electronic artifacts or instabilities of the separator can be easily detected. On the other hand, if the separator is set to $A/q < 2$, only fully stripped neutron-deficient isotopes can pass and no other isobars are available which would allow a monitoring of the intensity. Set to $A/q = 2$ for detection of $N = Z$ nuclei, a high background of scattered stable nuclides ^{12}C , ^{14}N and ^{16}O is present, especially at lower energies. Moreover, from trajectory calculations it is expected that neutron-deficient nuclei have very high average kinetic energies which would require voltages well beyond the maximum settings of the LOHENGRIN condenser. Thus, only the low-energy tail of the energy distribution can be probed and one has to rely on the predicted energy distribution to deduce a yield. To deduce the upper limits, an unfavorably high average kinetic energy was assumed in accordance with the trajectory calculations of ref.^{10,27}.

A dedicated set-up with a thick energy degrader foil mounted in front of the target to match the kinetic energy to the high-energy limit of the LOHENGRIN

^cThe use of the term "neutron-deficient" is here slightly extended to include also $N = Z$ nuclei. These are still "neutron-deficient" compared with the N/Z ratio of the compound nucleus.

Table 2: Experimental values for ^3He emission in ternary fission. For the spontaneous fission of ^{252}Cf upper limits of 50²⁸, 7.5²⁹ and 9³⁰ per 10000 LRA were reported.

Fissioning system	This work	³⁵	³⁴	³²	³¹	³³
$^{233}\text{U}(n_{\text{th}},f)$	< 0.018	< 0.1	≈ 180	-	-	-
$^{235}\text{U}(n_{\text{th}},f)$	< 0.008	-	-	< 0.01	< 0.08	-
$^{239}\text{Pu}(n_{\text{th}},f)$	-	-	-	-	-	< 0.01
$^{245}\text{Cm}(n_{\text{th}},f)$	< 0.6	-	-	-	-	-

spectrometer would allow an increase of the sensitivity by at least one order of magnitude.

^3He

Several older measurements gave upper limits for the fission yield of ^3He ^{28,29,30,31,32,33}, see table 2. Only in ref. ³⁴ a high yield for ^3He from $^{233}\text{U}(n,f)$ was reported: about 1.8 % of the LRA yield. However, this measurement was done with a simple $\Delta E-E$ telescope without additional particle separation. The alleged " ^3He " events are clearly due to scattered alphas which show up on the $\Delta E/E$ plot in the ^3He banana (see figure 4 in ³⁴).

With the present work the upper limits for the yield of ^3He from $^{235}\text{U}(n_{\text{th}},f)$ and $^{233}\text{U}(n_{\text{th}},f)$ could be confirmed and improved by a factor six in the latter case. Also for $^{245}\text{Cm}(n_{\text{th}},f)$ an upper limit could be given.

It should be noted that ^3He is particularly difficult to measure with the present LOHENGRIN set-up. Its expected average kinetic energy is above that of ^4He (≈ 15.9 MeV), presumably around 20 MeV. The fast ^3He ions cannot be fully stopped in the ionization chamber with the maximum permitted gas pressure. Thus, the much more abundant tritons which could pass the condenser during a short voltage fluctuation could appear on the $\Delta E/E$ plot close to the position of the expected ^3He events. Therefore the few events detected in the region of interest were only used to deduce an upper limit. A silicon detector for complete stopping and detecting of the E_r signal would help to improve the sensitivity.

^6Li , ^7Be and ^{10}B

For the isotopes ^6Li , ^7Be and ^{10}B only upper limits were found in the studied systems (see table 3). These results are consistent with the results from Gatchina ^{33,35,32}, only for ^6Li we find an upper limit below the value of ref.

Table 3: Experimental values for the emission of ${}^6\text{Li}$, ${}^7\text{Be}$ and ${}^{10}\text{B}$ in ternary fission.

Fissioning system	${}^6\text{Li}$	${}^7\text{Be}$	${}^{10}\text{B}$	Reference
${}^{233}\text{U}(n_{\text{th}},f)$	< 0.05	< 0.01	-	35
${}^{235}\text{U}(n_{\text{th}},f)$	0.05(2)	< 0.01	< 0.01	32
${}^{235}\text{U}(n_{\text{th}},f)$	1.04(27)	-	0.37(17)	10
${}^{235}\text{U}(n_{\text{th}},f)$	< 0.015	< 0.009	< 0.008	this work
${}^{239}\text{Pu}(n_{\text{th}},f)$	< 0.05	< 0.01	< 0.02	33
${}^{241}\text{Pu}(n_{\text{th}},f)$	-	< 0.2	< 0.03	this work
${}^{245}\text{Cm}(n_{\text{th}},f)$	< 0.3	-	< 0.3	this work

³². On the contrary, relatively high yields for ${}^6\text{Li}$ and ${}^{10}\text{B}$ were reported in ¹⁰. They had been corrected for contributions of scattered stable nuclei^d. Uncertainties in this correction can lead to a relatively big systematic error which was probably underestimated in ¹⁰.

Note that ${}^7\text{Be}$ would be an ideal candidate for a radiochemical investigation of ternary fission yields.

${}^{15}\text{O}$

A significant yield for ${}^{15}\text{O}$ from ${}^{235}\text{U}(n_{\text{th}},f)$ was reported in ⁹: 0.34(21) per 10000 LRA. Also in some of our measurements events showed up in the $\Delta E/E$ spectra which might be assigned to ${}^{15}\text{O}$. However, a more careful analysis showed that they are slightly shifted from the expected position on the $\Delta E/E$ plot. Such background could be created by ${}^{16}\text{O}$ from the residual gas being scattered in the beam tube and passing the spectrometer with a tilted trajectory at separator settings for mass 15. This explanation is supported by several facts:

1. The energy distribution does show a non-Gaussian behavior and rises significantly towards lower energies which is typical for scattered particles (see figure 5).
2. The yield of " ${}^{15}\text{O}$ " changes considerably between different measurements

^dParts of the ${}^6\text{Li}$ targets which have been introduced for on-line energy calibration of the LOHENGRIN separator²⁴, were sputtered off and deposited on the target holder. Therefore a permanent background of scattered ${}^6\text{Li}$ as well as alphas and tritons from ${}^6\text{Li}(n,\alpha)$ is present at lower energies.

with the same fissioning system. It showed a correlation with the vacuum conditions in the beam tube (increase of the "yield" with bad vacuum).

- Moreover, the ionic charge state distribution of ^{15}O events deviates from that for ternary oxygen isotopes. The same effect occurs for other scattered stable particles. Obviously the equilibrium charge state is not reached in a single scattering process.

Using only the points above 20 MeV together with an average energy consistent with the trajectory calculations of 10,27 , upper limits were deduced from the present measurements: 0.013 in $^{233}\text{U}(n_{\text{th}},f)$, 0.016 in $^{235}\text{U}(n_{\text{th}},f)$ and 0.12 in $^{241}\text{Pu}(n_{\text{th}},f)$ per 10000 LRA, respectively.

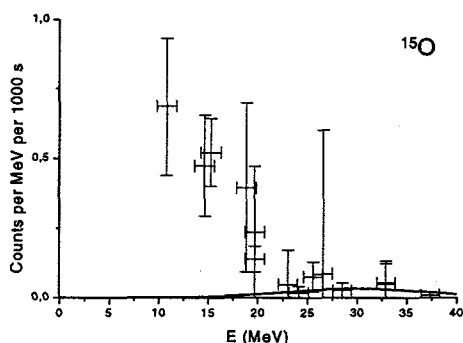


Figure 5: Energy distribution of alleged ^{15}O events in thermal neutron-induced fission of ^{233}U . The rise towards lower energies indicates a large contribution of scattered ^{16}O .

It can be summarized that presently in low-energy fission only upper limits exist for the experimental yields of all neutron-deficient ternary particles. Most models of ternary fission yields fail to predict the very sharp drop of the yields towards small N/Z ratio.

Mutterer et al. have shown that ^5He and ^7He are also emitted in ternary fission and follow a smooth exponential drop towards higher masses without markable neutron odd-even effect³⁶. Therefore it is even more astonishing why for ^3He such an abrupt drop occurs.

Yield of very neutron-rich nuclei

From the experimental results it is evident that the yields of very neutron-rich light nuclei are considerably smaller than most model predictions. Before interpreting this fact as a clear model failure it has to be checked whether other effects could cause such a deviation. It is clear that the N/Z ratios of

exotic isotopes differ strongly from that of the fissioning compound nucleus. Such nuclei are intuitively expected to be created with a lower yield. However, this effect is already assumed to be included in the presented models which are generally applicable to *all* ternary particles.

Suppression of halo nuclei?

Another effect could occur for very neutron-rich nuclei. If the binding energy for the last neutron(s) S_{zn} is very low, some nuclides show a so-called neutron halo. That means the wave function of the weakly bound valence neutrons has a tail which extends far away. Therefore the mean square matter radius and the nuclear cross-section for breakup are significantly increased.

The possibility of a halo depends on the neutron separation energy S_{zn} and the angular momentum of the "halo" neutron(s). As a rule of thumb a halo can appear if S_{zn} is smaller than approximately $5 - 10 \text{ MeV fm}^2/R^2$, where R is the radius of an equivalent square well potential³⁷. Among the studied ternary particles, ^{11}Be and ^{19}C are known to have a one-neutron halo, ^6He , ^{11}Li , ^{14}Be and ^{17}B have a two-neutron halo and ^8He can be described by an alpha core with a four-neutron halo³⁸. Table 4 gives a summary of the binding energies of the last neutron(s).

Table 4: Binding energies of the halo neutrons in neutron-halo nuclei. Where no reference is given they were calculated from the atomic mass evaluation of Audi and Wapstra³⁹.

Isotope	S_{1n} MeV	S_{2n} MeV	S_{4n} MeV	Reference
^6He		0.973(1)		
^8He		2.139(7)	3.112(7)	
^{11}Li		0.30(3)		
^{11}Be	0.504(6)			
^{14}Be		1.34(12)		
^{17}B		1.39(15)		
^{19}C	0.25(9) ^e			40

For kinetic energies far below the Coulomb barrier as in our case, Coulomb breakup of the ternary particles while passing the target can be neglected. Also, the dissociation of the halo nucleus in a scattering reaction is negligible in the thin target. The only process which could cause a significant effect is the breakup of the halo while the ternary particle is exposed to the strong

^eRecent results indicate a higher value of $S_n = 0.53(13)$ ⁴¹.

Table 5: Yield ratios of halo nuclei and well-bound isotopes. Only in two systems the ratio of ^{15}B to ^{17}B has been measured: > 140 for $^{235}\text{U}(n_{\text{th}},f)$ and > 36 for $^{241}\text{Pu}(n_{\text{th}},f)$.

Fissioning system	$\frac{^4\text{He}}{^6\text{He}}$	$\frac{^6\text{He}}{^8\text{He}}$	$\frac{^7\text{Li}}{^9\text{Li}}$	$\frac{^9\text{Li}}{^{11}\text{Li}}$	$\frac{^9\text{Be}}{^{11}\text{Be}}$	$\frac{^{10}\text{Be}}{^{12}\text{Be}}$	$\frac{^{12}\text{Be}}{^{14}\text{Be}}$
	$^{233}\text{U}(n_{\text{th}},f)$	73(4)	38(5)	1.0(2)	11500(9000)	1.9(11)	39(8)
$^{235}\text{U}(n_{\text{th}},f)$	52(3)	23(3)	1.1(1)	3300(900)	1.2(3)	23(2)	3600(2200)
$^{239}\text{Pu}(n_{\text{th}},f)$	52(2)	22(2)	1.2(1)	3100(1200)	1.5(3)	22(6)	5600(3700)
$^{241}\text{Pu}(n_{\text{th}},f)$	38(4)	17(3)	0.81(11)	1800(700)	0.75(23)	16(3)	1000(400)
$^{245}\text{Cm}(n_{\text{th}},f)$	35(3)	15(3)	1.0(2)	1400(900)	1.1(2)	12(2)	310(210)

Table 6: Yield ratios of halo nuclei and well-bound isotopes.

Fissioning system	$\frac{^{14}\text{C}}{^{16}\text{C}}$	$\frac{^{15}\text{C}}{^{17}\text{C}}$	$\frac{^{16}\text{C}}{^{18}\text{C}}$	$\frac{^{17}\text{C}}{^{19}\text{C}}$	$\frac{^{18}\text{C}}{^{20}\text{C}}$	$\frac{^{20}\text{O}}{^{22}\text{O}}$
	$^{233}\text{U}(n_{\text{th}},f)$	6.0(10)	-	40(11)	-	-
$^{235}\text{U}(n_{\text{th}},f)$	6.1(9)	8.3(12)	25(7)	-	9(4)	26(11)
$^{241}\text{Pu}(n_{\text{th}},f)$	2.5(5)	6.7(17)	18(5)	260(160)	78(63)	9.2(32)
$^{245}\text{Cm}(n_{\text{th}},f)$	2.5(9)	12(5)	30(15)	> 15	> 4	7.0(35)

nuclear and Coulomb forces when the neck is snapping and all three fragments are accelerated. The magnitude of this effect, however, is extremely dependent on all details of the scission configuration. The missing knowledge on the scission configuration already causes most of the uncertainties in the predictions of the ternary fission models discussed above. Thus, a quantitative treatment of this additional effect does not make sense. Nevertheless, it can be qualitatively checked whether a major influence on the yields could occur. For different ternary particles which are created in similar scission configurations, the breakup probability should show a strong dependence on S_{xn} . The effect would be more pronounced for isotopes with a weak binding of the last neutrons. The problem is to find a suitable normalization for such a comparison. To avoid biasing by proton- or neutron-odd-even effects, the ratio of the yield of the isotope $^{A-2}_Z X$ to the yield of $^A_Z X$ can be regarded. Thus, the influence of the proton- and neutron pairing energy should mainly cancel^f. Tables 5 and 6 show experimental values of the yield ratios for several pairs of nuclei.

In the case of carbon, the yields of directly neighboring nuclei can be

^fThis situation is similar to that of nuclear mass models. For a comparison often the S_{2n} or S_{2p} values are plotted. This removes the staggering due to pairing effects.

Table 7: Yield ratios of halo nuclei and well-bound isotopes.

Fissioning system	$\frac{[^{15}\text{C}]}{[^{16}\text{C}]}$	$\frac{[^{17}\text{C}]}{[^{18}\text{C}]}$	$\frac{[^{19}\text{C}]}{[^{20}\text{C}]}$	$\frac{[^{10}\text{Be}]}{[^{11}\text{Be}]}$	$\frac{[^{14}\text{C}]}{[^{15}\text{C}]}$	$\frac{[^{20}\text{O}]}{[^{21}\text{O}]}$
$^{233}\text{U}(\text{n}_{\text{th}},\text{f})$	1.1(3)	–	–	22(12)	5.2(8)	23(7)
$^{235}\text{U}(\text{n}_{\text{th}},\text{f})$	1.2(2)	3.6(10)	–	12(2)	5.3(2)	8.5(28)
$^{239}\text{Pu}(\text{n}_{\text{th}},\text{f})$	1.0(6)	–	–	14(2)	4.0(15)	–
$^{241}\text{Pu}(\text{n}_{\text{th}},\text{f})$	0.9(2)	2.3(7)	0.7(7)	7.8(25)	2.9(4)	4.8(14)
$^{245}\text{Cm}(\text{n}_{\text{th}},\text{f})$	0.8(3)	2.0(9)	–	8.1(12)	3.0(5)	3.8(14)

compared. Also for the odd- N isotope ^{11}Be a different ratio is chosen for comparison. These ratios are shown in table 7. They are influenced by the neutron-pairing energy. However, the relative influence should be small since identical ratios are regarded: i.e. (o,e)- versus (e,e)- and (e,e)- versus (e,o)- nuclei.

The ratios presented in tables 5 and 6 have been calculated from the values measured in this work. Other values were taken from^{35,42} for $^{233}\text{U}(\text{n}_{\text{th}},\text{f})$, from¹⁰ for $^{235}\text{U}(\text{n}_{\text{th}},\text{f})$ and from³³ for $^{239}\text{Pu}(\text{n}_{\text{th}},\text{f})$.

Table 5 shows clearly a more pronounced drop towards heavier isotopes for lithium and beryllium compared with helium, carbon and oxygen nuclei. However, from table 7 it can be seen that the other halo nuclei ^{11}Be and ^{19}C do not show such a significant reduction. If a suppression of halo nuclei occurs for ^{11}Li and ^{14}Be , it should also be present in comparable magnitude for the latter nuclei. Thus, it cannot be excluded that halo nuclei are possibly “suppressed” by up to 50 %, but this effect is not able to explain deviations of one order of magnitude and more.

To decide why the models fail to explain the yield drop for exotic lithium and beryllium nuclei, the difference in “energy costs” has to be analyzed in more detail. As explained before, the influence of the pairing energy is mainly removed⁹ by the choice of these yield ratios. In the double-neck-rupture model and the Boltzmann model the Coulomb energy is practically constant for different isotopes of one element^h. However, in the parameterization of the other models the fragment distance depends strongly on the ternary particle mass. Therefore, for the considered nuclei the difference in Coulomb energy $E_{\text{Coul}}^{\text{TP}}(A-2, Z, X) - E_{\text{Coul}}^{\text{TP}}(A, Z, X)$ attains about 1.5 MeV in the extended Halpern

⁹Only in the Boltzmann model the pairing energy is explicitly included. For the discussed yield ratios the difference $E_{\text{Coul}}^{\text{TP}}(A-2, Z, X) - E_{\text{Coul}}^{\text{TP}}(A, Z, X)$ will attain up to 5 MeV, but this can be due to the somehow artificial parameterization of the pairing energy.

^h $E_{\text{Coul}}^{\text{TP}}(A-2, Z, X) - E_{\text{Coul}}^{\text{TP}}(A, Z, X) \leq 0.3$ MeV.

model¹⁵ and even higher values for the two other models^{10,11}. Still the dominant contribution to the energy costs comes from the reaction Q-value. Figure 6 shows a plot of the yield ratios $[^{A-2}_Z X]/[^A_Z X]$ from tables 5 and 6 versus the Q-value difference $\Delta Q = Q(^{A-2}_Z X) - Q(^A_Z X)$. The Q-value difference was calculated with the heavy fragment fixed to ^{132}Sn .

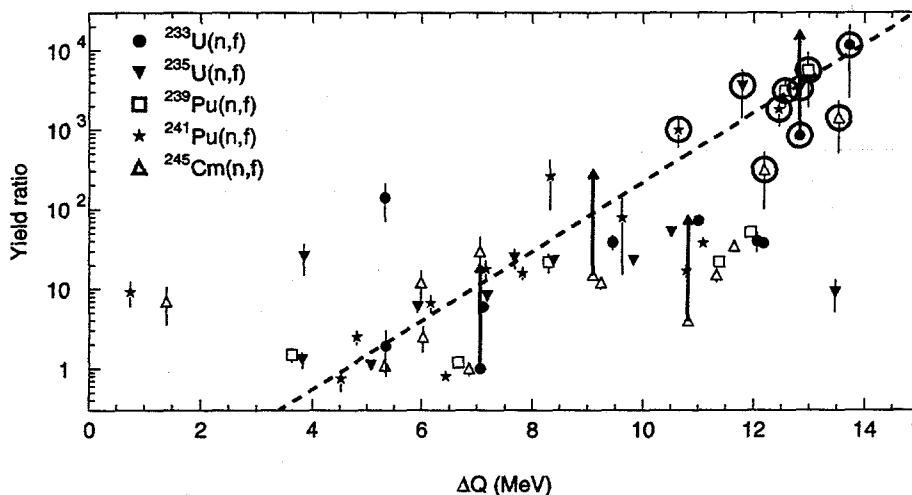


Figure 6: Yield ratios $[^{A-2}_Z X]/[^A_Z X]$ versus the Q-value difference. Arrows indicate lower limits of the yield ratio. The values of $[^9\text{Li}]/[^{11}\text{Li}]$ and $[^{12}\text{Be}]/[^{14}\text{Be}]$ are marked with a ring around. For comparison an exponential function $y = 0.01 \cdot \exp(\Delta Q/1 \text{ MeV})$ is shown as dashed line.

Despite a significant scattering of the values, the dependence of the yields on the Q-value is apparent. The dashed line shows an exponential dependence with a parameter $T = 1 \text{ MeV}$ in formula (1)⁴. This is significantly lower than the T parameter used in all discussed ternary fission models (compare table 1)! For a detailed analysis each fissioning system has to be studied specifically, including the features of the individual models (influence of the Coulomb and correction energies) and the yields of very heavy ternary particles.

It can be concluded that the present models of ternary fission fail to predict the strong decrease of yields for light exotic nuclei. This disagreement cannot be easily removed by "tuning" a single model parameter. Possibly the basic assumption of a direct exponential dependence of the yields on the energy costs holds no longer good for very unfavorable mass splits.

⁴This is not a real fit, but just an illustration of the qualitative dependence of several fissioning systems.

Acknowledgments

This work was partly supported by the U.S. Department of Energy, Nuclear Physics Division, contract No. W-31-109-ENG-38. The authors are also indebted for the use of ^{245}Cm to the Office of Basic Energy Sciences, U.S. Department of Energy, through the transplutonium element production facilities at Oak Ridge National Laboratory. We thank Prof. Johannes-Otto Denschlag and Dr. Norbert Trautmann (Institut für Kernchemie, Universität Mainz) for the preparation of the ^{245}Cm targets. Thanks for support by the Accelerator Laboratory of the TU and LMU München.

References

1. T. San-Tsiang *et al.*, C. R. Acad. Sci. Paris 223 (1946) 986.
2. G. Farwell, E. Segrè and C. Wiegand, Phys. Rev. 71 (1947) 327.
3. F. Gönnenwein, Pont d'Oye IV, 1999, these proceedings.
4. B. Wilkens, E. Steinberg and R. Chasman, Phys. Rev. C 14 (1976) 1832.
5. U. Brosa, S. Grossmann and A. Müller, Phys. Rep. 197 (1990) 167.
6. G. Val'skiĭ, Sov. J. Nucl. Phys. 24 (1976) 140.
7. V. Rubchenya and S. Yavshits, Z. Phys. A 329 (1988) 217.
8. V. Rubchenya, priv. comm.
9. W. Baum *et al.*, *6th Int. Conf. on Nuclei far from Stability & 9th Int. Conf. on Atomic Masses and Fund. Const.*, Bernkastel-Kues, ed. by R. Neugart and A. Wöhr, Inst. Phys. Conf. Ser. No. 132, IOP, Bristol, 1992, p. 477.
10. W. Baum, Ph.D. thesis, TH Darmstadt, 1992.
11. G. Pik-Pichak, Phys. At. Nucl. 57 (1994) 906.
12. H. Faust and Z. Bao, in *Proc. Seminar on Fission, Pont d'Oye III*, ed. by C. Wagemans, 1995, p. 220.
13. H. Faust, in *Proc. Seminar on Fission, Pont d'Oye III*, ed. by C. Wagemans, 1995 p. 211.
14. F. Gönnenwein *et al.*, *6th Int. Conf. on Nuclei far from Stability & 9th Int. Conf. on Atomic Masses and Fund. Const.*, Bernkastel-Kues, ed. by R. Neugart and A. Wöhr, Inst. Phys. Conf. Ser. No. 132, IOP, Bristol, 1992, p. 453.
15. M. Wöstheinrich, M. Hesse and F. Gönnenwein, in *Dynamical Aspects of Nuclear Fission, Proc. of 3rd Int. Conf. held at Častá-Papiernička*, ed. by J. Kliman and B. Pustynnik, JINR, Dubna, 1996, p. 231.
16. I. Halpern, Annu. Rev. Nucl. Sci. 21 (1971) 245.
17. A. Gavron, Phys. Rev. C 11 (1975) 580.

18. F. Gönnewein and B. Börsig, Nucl. Phys. A 530 (1991) 27.
19. V. Rubchenya, A. Roschin and S. Yavshits, in *Workshop on Nuclear Fission and Fission-Product Spectroscopy, Seyssins*, ed. by H. Faust and G. Fioni, Institut Laue Langevin, report 94FA05T, 1994, p. 26.
20. R. Bass, *Lecture notes in physics: Deep-inelastic and fusion reactions with heavy ions*, vol. 117, Springer, Berlin, 1980, p. 281.
21. B. Börsig, Ph.D. thesis, Universität Tübingen, 1993.
22. M. Hesse, Ph.D. thesis, Eberhard-Karls-Universität Tübingen, 1997.
23. M. Wöstheinrich *et al.*, Acta Phys. Slovaca 49 (1999) 117.
24. U. Köster *et al.*, Nucl. Phys. A 652 (1999) 371.
25. U. Köster, Master's thesis, TU München, 1995.
26. U. Köster, Ph.D. thesis, TU München, to be published.
27. B. Bouzid, Ph.D. thesis, Université des sciences et de technologie Houari Boumedienne, Alger, 1994.
28. H. Wegner, Bull. Am. Phys. Soc. 6 (1961) 307.
29. S. Cosper, J. Cerny and R. Gatti, Phys. Rev. 154 (1967) 1193.
30. S. Whetstone and T. Thomas, Phys. Rev. 154 (1967) 1174.
31. G. Kugler and W. Clarke, Phys. Rev. C 5 (1972) 551.
32. A. Vorobyov *et al.*, Phys. Lett. 40B (1972) 102.
33. A. Vorob'ev *et al.*, Sov. J. Nucl. Phys. 20 (1975) 248.
34. M. Cambiaghi, F. Fossati and T. Pinelli, Il Nuovo Cimento LIX B (1969) 236.
35. A. Vorobiev *et al.*, Phys. Lett. 30B (1969) 332.
36. M. Mutterer *et al.*, Pont d'Oye IV, 1999, these proceedings.
37. K. Riisager, A. Jensen and P. Möller, Nucl. Phys. A 548 (1992) 393.
38. M. Zhukov, A. Korshennikov and M. Smedberg, Phys. Rev. C 50 (1994) R1.
39. G. Audi and A. Wapstra, Nucl. Phys. A 595 (1995) 409.
40. B. Jonson, *Exotic Nuclei and Atomic Masses, ENAM'98, Bellaire, Michigan, June 1998*, ed. by B. Sherill, D. Morrissey and C. Davids, AIP Conf. Proc. 455, Woodbury, NY, 1998, p. 166.
41. T. Nakamura *et al.*, *Exotic Nuclei and Atomic Masses, ENAM'98, Bellaire, Michigan, June 1998*, ed. by B. Sherill, D. Morrissey and C. Davids, AIP Conf. Proc. 455, Woodbury, NY, 1998, p. 215.
42. M. Wöstheinrich *et al.*, *Nuclear Fission and Fission-Product Spectroscopy, Second Int. Workshop, Seyssins, France, 1998*, ed. by G. Fioni *et al.*, AIP Conf. Proc. 447, 1998, p. 330.